# Retrograde flow rate is increased in growth cones from myosin IIB knockout mice

**Michael E. Brown and Paul C. Bridgman***

Washington University School of Medicine, Department of Anatomy and Neurobiology, Box 8108, 660 S. Euclid Avenue, St Louis, MO, USA
*Author for correspondence (e-mail: bridgmap@pcg.wustl.edu)

*Accepted 21 December 2002*
*Journal of Cell Science 116, 1087-1094 © 2003 The Company of Biologists Ltd*
*doi:10.1242/jcs.00335*

## Summary

**Growth cones of myosin-IIB-knockout mice have reduced outgrowth rates and traction force. There is a close relationship between traction force, retrograde flow and forward advance of growth cones. All three activities appear to be at least partially myosin dependent. Therefore, we have now tested for differences in retrograde flow rates between growth cones from myosin-IIB-knockout mice and their normal littermates. By placing nerve-growth-factor-coated silica beads on the surface of growth cones with laser tweezers, or by tracking GFP-myosin IIA spots, we found that the retrograde flow rate was increased more than two fold in the knockout growth cones compared with the wild type. These data suggest that both myosin IIA and IIB normally contribute to retrograde flow and the properties of the flow are strongly influenced by myosin IIB because of its location and abundance. However, in the absence of myosin IIB, myosin IIA takes over this function. The change in retrograde flow rate may reflect the difference in functional properties of these two myosins. Knockout growth cones also exhibited reduced stability of lamellipodia, possibly as a partial consequence of this increased retrograde flow rate. In addition, microtubules penetrated a shorter distance into filopodia, which suggests that the increase in flow rate may adversely affect the microtubule-dependent maturation of filopodia. Taken together these data support the idea that the forward advance of the growth cone is myosin II dependent and involves multiple myosin II isoforms.**

Key words: Actin, Nerve outgrowth, Motility

## Introduction

The leading edge of motile cells has specialized actin rich structures: lamellipodia and filopodia. It has been shown through numerous studies that the actin cytoskeleton of lamellipodia and filopodia undergo retrograde flow relative to the substrate during forward movement (Forscher and Smith, 1988; Fisher et al., 1988; Danuser and Oldenbourg, 2000; Salmon et al., 2002). The exception is rapidly moving cells such as fish keratocytes that have a stationary actin cytoskeleton during advance (Theriot and Mitchison, 1991). The difference between keratocytes and most other cell types appears to reside in the coupling between the actin cytoskeleton and the substrate. In most cells there is 'slippage' between the rearward movements of the actin cytoskeleton and the forward advance of the cell so that actin moves rearward faster than the cell advances forward (Suter et al., 1998). The coupling between the actin cytoskeleton and the surface of the cell can be observed by placing beads or particles coated with various materials on the surface of the cell (Dembo and Harris, 1981; Lin and Forscher, 1995). Cells that show retrograde flow also show the rearward movement of beads at the same rate as the movement of the actin cytoskeleton (Lin and Forscher, 1995). The mechanism driving both forward advance and the retrograde flow of the actin cytoskeleton appears to be the same because they show an inverse relationship (Lin and Forscher, 1995). The force driving these activities appears to be myosin based (Lin et al., 1996), although in some cells types actin polymerization may also contribute (Henson et al., 1999).

Growth cones, similar to other motile cells, exhibit retrograde flow of actin, and beads applied to their surface move rearward (Lin and Forscher, 1995; Lin et al., 1996). It has been shown that inhibition of myosin activity results in disruption of retrograde flow in growth cones (Lin et al., 1996). However, the identity of the myosins involved remains unknown, although a recent report has suggested the involvement of myosin IC (Diefenbach et al., 2002). It remains to be determined whether or not multiple types of myosin contribute to retrograde flow. A number of different cell types have been used to study retrograde flow in growth cones, but the myosins present have not been fully identified. As a result of the data compiled from the human genome project, it now appears that mammalian cells have three types of myosin II. Two types of myosin II (A and B) have been identified in nerve growth cones (Rochlin et al., 1995), and it is possible that a third type is also present (Berg et al., 2001). Myosin IIB is the only isoform that appears to be enriched in neurons compared with other cell types (Rochlin et al., 1995).

Recently we showed that neurons grown in cell culture from a myosin IIB knockout mouse exhibited slowed outgrowth rates (Tullio et al., 2001). Growth cones showed altered actin organization, size and motility (Bridgman et al., 2001). In addition, filopodia-dependent traction force, which is thought to contribute to forward advance of the growth cone, was reduced. Since there is a close relationship between traction force and retrograde flow, we have now tested for differences in retrograde flow rates between growth cones from myosin-

IIB-knockout (KO) mice and their normal littermates. We find that the retrograde flow rate is significantly increased more than two fold in the KO growth cones compared with wild type (wt). KO growth cones also exhibited reduced stability of lamellipodia, which may be a consequence of this increased flow rate. In addition, microtubules penetrated a shorter distance into filopodia. These results suggest that both myosin IIA and IIB contribute to retrograde flow and traction force. In the absence of myosin IIB, myosin IIA alone may take over these functions, and the increased rate of retrograde flow mainly reflects the properties of this myosin. The increase in flow rate may also adversely affect the microtubule-dependent maturation of filopodia. This supports the idea that forward advance of the growth cone is myosin II dependent and involves multiple myosin II isoforms.

## Materials and Methods

### Cell culture

Superior cervical ganglion neurons were cultured from E13.5-E14.5 mouse embryos as previously described (Bridgman et al., 2001). The identity of the myosin-IIB-knockout embryos was tentatively made using the distorted head shape that results from hydrocephalus (Tullio et al., 1997; Tullio et al., 2001). The identity was then confirmed by western blot analysis of brain tissue. Genotypes were subsequently determined by Southern blot analysis of tails (Bridgman et al., 2001).

### Microscopy and laser trapping

A laser tweezers was constructed using a SDL 500 mW diode laser emitting at 835 nm and an Olympus IX70 microscope as described by Fallman and Axner (Fallman and Axner, 1997). Cells were imaged with a Cooke Sensicam digital camera using DIC microscopy. Time-lapse sequences were captured using Scanalytics IpLab. Measurements on digital images were also performed using IpLab. A filopodium was defined as a long narrow structure uniform in diameter or slightly tapering towards the tip arising from the growth cone perimeter. A lamellipodium was defined as a broad protrusive structure arising from the growth cone perimeter. Filopodium-like structures were defined as long, narrow structures that contained small branches or flaring tips. All structures were enriched in actin when appropriately stained. We restricted our quantitative analysis to the more labile population of protrusive structures at the leading edge (approximately the distal one-third of the cone). A flow chamber was used for experiments to allow delivery of nerve growth factor (NGF)-coated beads. For most experiments, cells were first equilibrated with low NGF medium prior to introducing NGF-coated beads (Gallo et al., 1997).

### Immunostaining

For comparison of microtubules, actin and myosin IIA, cells were fixed and stained as previously described using method 1 (Rochlin et al., 1995). Rhodamine phalloidin was used to stain actin. An affinity-purified polyclonal antibody to rodent myosin IIA was used to detect myosin IIA (Rochlin et al., 1995). A rat monoclonal antibody to tyrosinated tubulin was used to detect distal microtubule segments.

For comparison of myosin IIA and myosin IC staining, two fixation methods were used. The first was 4% paraformaldehyde (EM grade) in 0.1 M cacodylate buffer, and the second was rapid immersion in cold methanol (–20°C). The staining patterns were identical, although the first method gave a slightly higher diffuse background in thickened regions. The myosin IC monoclonal antibody (m2) was a gift of J. Albanesi.

Immunofluorescence images were taken using a slow scan CCD (Roper Scientific Series 300). Figures were prepared using Adobe Photoshop. Contrast in photographs was enhanced using the unsharp mask filter.

### Preparation of beads

Carboxylated silica beads (1.5 μm, Bangs Laboratories) were linked to NGF following published protocols (Gallo et al., 1997).

### Biolistics

A custom-designed gene gun (Bridgman et al., 2003) was used to introduce a GFP-myosin IIA cDNA into cultured control and KO SCG neurons. The GFP was fused to the N-terminus of the myosin IIA heavy chain using the pEGFP-C3 vector (Clontech) as previously described (Wei and Adelstein, 2000), except that the pTRE promoter was replaced with the cytomegalovirus promoter.

## Results

Laser tweezers were used to trap 1.5 μm NGF-coated silica beads and maneuver them into a position just above the growth cone peripheral (P) domains. The trap was shut off and the beads were allowed to settle on to the growth cone surface. In the presence of soluble NGF, the beads did not bind to the growth cone surface but diffused away (22/22 trials). In low soluble NGF medium the beads bound to the growth cone surface in 42% (52/124) of the trials. The binding could be categorized into two distinct behaviors. In the first, the beads appeared to bind loosely. They made relatively rapid movements in all directions within the plane of the membrane surface. When new extensions developed, the loosely bound beads tended to make net movements outward with the extension. When the periphery retracted, the beads made net movements inwards with the retracting process. Movements continued even within the central domain of the cone. The second category appeared to result in tighter binding. The beads did not make rapid movements, but if the binding occurred in the peripheral domain the beads moved slowly rearward. The net movement ceased when the beads had moved into or settled in the central domain. Both categories of movement were observed in wt and KO growth cones, and we presume they represent two different states of interaction with the Trk A receptor (Gallo et al., 1997; Thoumine and Meister, 2000). We have only analyzed the slower retrograde movement in detail because it is thought to reflect the behavior of the actin cytoskeleton (Lin and Forscher, 1995). Aminated or laminin-coated beads also underwent retrograde flow similar to NGF-coated beads, but they also tended to aggregate and sometimes induced ‘inductopodia’ (Forscher et al., 1992).

To determine the rate of retrograde bead movement, we took time-lapse images at 6.5 second intervals (Fig. 1A,B). We then tracked the bead centroid position over multiple frames. Graphs of net displacement over time indicated that the bead displacement in the peripheral domain was approximately linear over relatively short time periods in both wt and KO growth cones (Fig. 1C,D). Movement varied in rate depending on bead position, but in general progressively slowed as beads approached the central domain. Linear regression was used to calculate the slope of the bead displacement curve at its steepest point, and this value was used as the maximum rate of bead movement. Comparison of rates in wt and KO cones indicated that there was some variation in the rates of

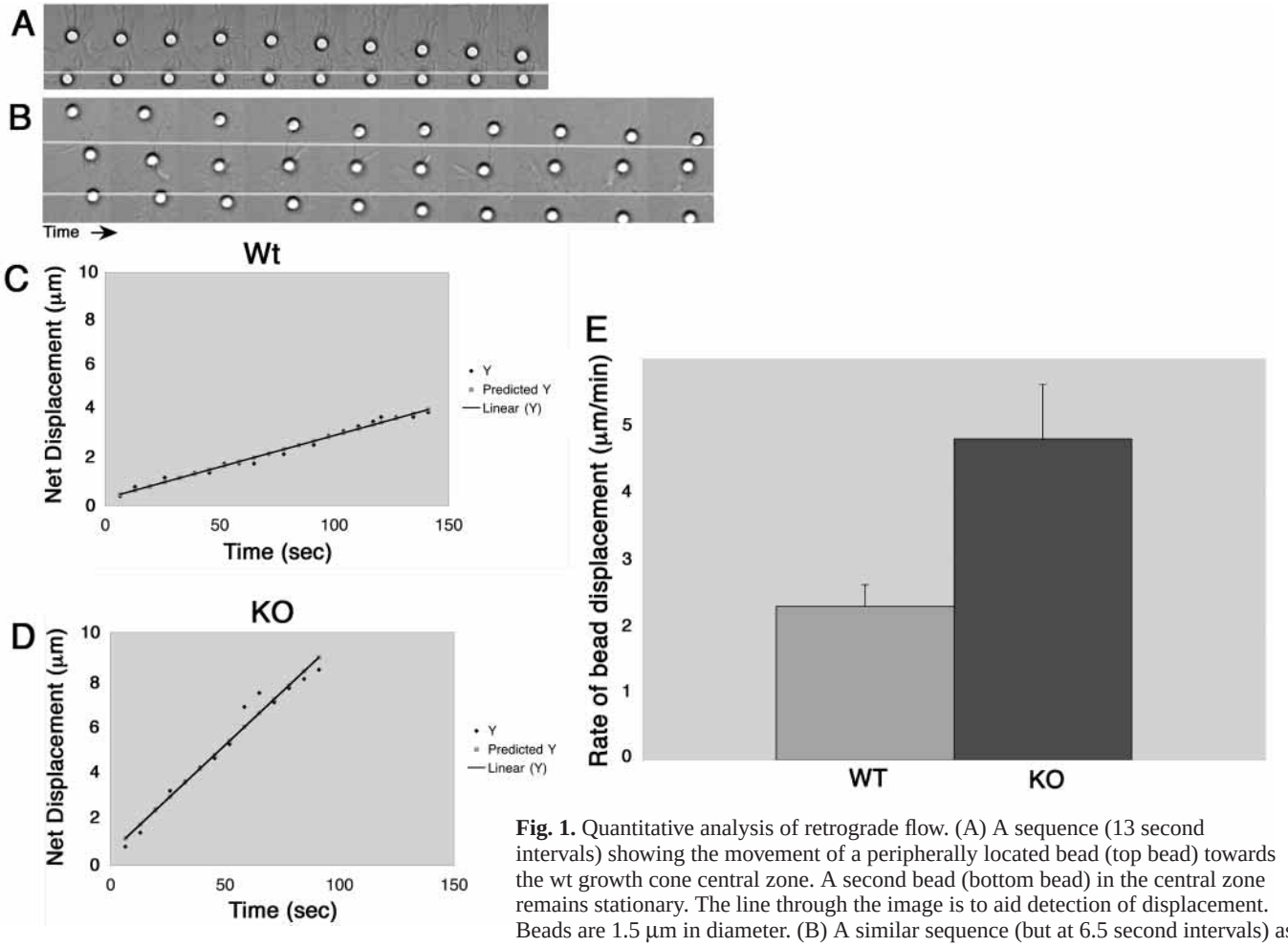


**Fig. 1.** Quantitative analysis of retrograde flow. (A) A sequence (13 second intervals) showing the movement of a peripherally located bead (top bead) towards the wt growth cone central zone. A second bead (bottom bead) in the central zone remains stationary. The line through the image is to aid detection of displacement. Beads are 1.5 μm in diameter. (B) A similar sequence (but at 6.5 second intervals) as in A, from a KO growth cone. Three beads are undergoing rearward movement (towards the bottom of the image) independently of a single growth cone. (C) Regression analysis of the steepest portion of a bead displacement versus time curve from a wt cone. The slope of the regression line was used as the maximum rate of bead displacement. (D) The same analysis as in C, but from a KO cone. Note that in general KO cones showed slightly more deviation from linearity (lower $r^2$ values) than wt. (E) Comparison of wt and KO maximum rates of bead displacement ($n$=10 for each). The difference was significant ($t$-test, $P$<0.01).

movement between different growth cones for both. However, the average maximum rate of movement in wt cones was significantly different from in KO cones ($t$-test, $P$<0.01). The rate of retrograde movement in KO cones was on average 2.1 times faster than the movement in wt cones (Fig. 1E).

Although there is good evidence that the rate of retrograde bead movement on growth cones closely reflects the rate of retrograde flow of the actin cytoskeleton, we wanted to verify this result in our system. To do this, we expressed GFP–myosin-IIA in control and KO neurons. There is good evidence that myosin II forms small bipolar filaments in lamellipodia of motile cells, and the behavior of these minifilaments reflects the dynamics of the actin cytoskeleton to which they are attached (Svitkina et al., 1997). GFP–myosin-IIA has been shown to incorporate into F-actin-rich structures that normally are associated with myosin IIA in noneuronal cells, such as stress fibers, indicating that it is correctly targeted (Wei and Adelstein, 2000) (P.C.B., unpublished). In both wt and KO growth cones, GFP–myosin-IIA appeared as small fluorescent spots (Fig. 2A). These spots were labile, they often appeared and disappeared within minutes and also changed intensity. We assume that these spots represent small bipolar filaments that have been observed in both noneuronal cells and growth cones (Svitkina et al., 1997; Bridgman, 2002). In peripheral regions of the growth cone, spots consistently appeared and then (usually) underwent retrograde flow. The moving spots often slowed their rate of movement, merged and accumulated into linear arrays within the transition zone. We tracked a subset (those that could be identified for at least three frames) of spots by time-lapse imaging to determine their rate of movement (Fig. 2B). The average rates of spot movement for both wt and KO were about the same as the average rates of bead movement (compare Fig. 1C with Fig. 2C). Again, as was observed for bead movement, the retrograde movement of spots in KO growth cones was little over twice (2.3×) the rate of movement in wt cones. The difference was significant ($t$-test, $P$<0.001). This indicates that the NGF-coated beads can act as an accurate marker for the retrograde flow of the actin cytoskeleton and that KO growth cones have an increased rate of retrograde flow.

There is good evidence from experiments using neuroblastoma cells to suggest that the dynamics of filopodia

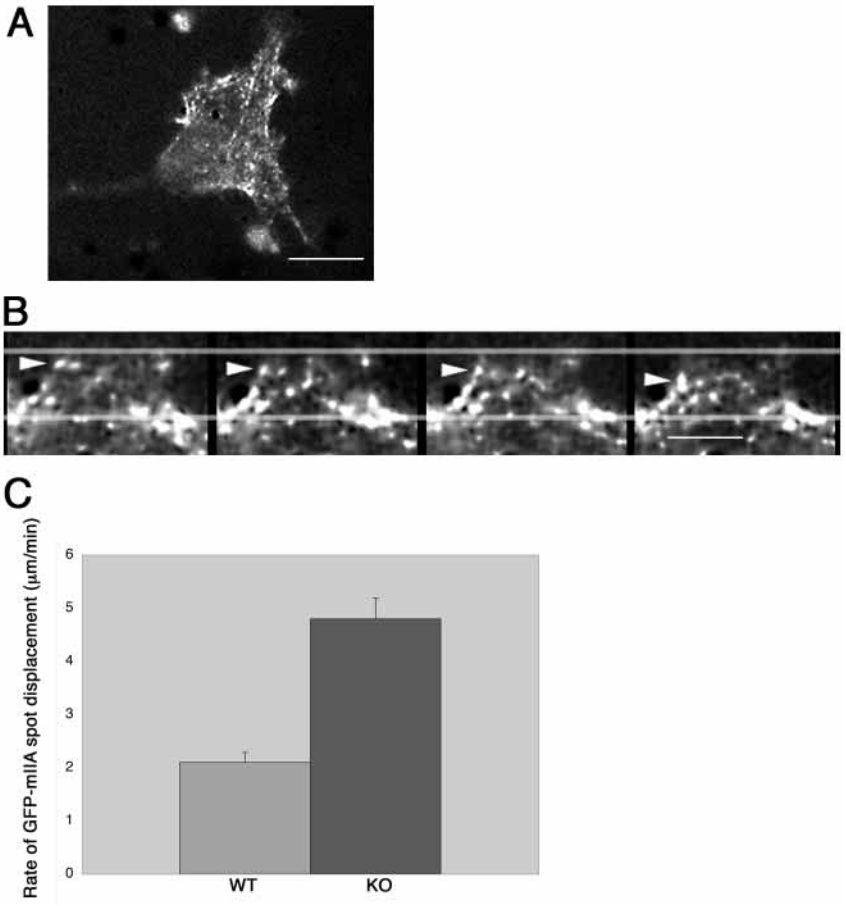


**Fig. 2.** Tracking retrograde flow using GFP–myosin-IIA fluorescent spots. (A) A KO growth cone from a SCG neuron expressing GFP–myosin-IIA (the barely visible neurite is on the left side of the field). The spots of fluorescence sometimes align presumably along actin bundles. (B) A high magnification sequence from the KO cone showing the displacement of spots (the pair indicated by the arrowhead) over time. The lines through the images are for position reference and allow one to see the retrograde displacement (from top to bottom of image). Because many of the spots changed intensity, appeared and disappeared at different times, only a subset of spots could be identified with certainty in multiple frames. The elapsed time between images is 13 seconds. (C) Comparison of the average rate (±s.e.m.) of GFP–myosin-IIA spot displacement from wt and KO growth cones. The spots in the KO growth cones ($n$=11) move more than twice the speed of those in the wt ($n$=15). The individual rates were calculated from the total distance that spots moved over a minimum of three frames divided by the elapsed time (13 second intervals). A, bar, 12 μm; b, bar, 2 μm.

and lamellipodia result from the balance between retrograde flow and actin polymerization (Mallavarapu and Mitchison, 1999). Cessation of actin polymerization usually results in retraction because of the action of retrograde flow. When the rates of actin polymerization and retrograde flow are matched, no change occurs. However, if the actin polymerization rate exceeds the rate of retrograde flow then protrusion occurs. Actin polymerization and retrograde flow appear to be independently regulated. Because the retrograde flow rate is increased in the KO growth cones, we wanted to know if this had an affect on protrusion and retraction rates. Therefore we used time-lapse images (Fig. 3) to measure the rates of both filopodia retraction and protrusion. Although the average rate of KO protrusions was slightly less than that of wt (wt=3.3±0.34 μm/minute, $n$=16, KO=2.8±0.3 μm/minute, $n$=16, s.e.m.), the difference was not significant. Similarly, the average rates of retractions were the same (wt=9.8±1.7 μm/minute, $n$=16, KO=10±2.2 μm/minute, $n$=16). Thus there is no detectable difference in the average rates of protrusion or retraction of filopodia between KO and wt.

Previously we observed an increased frequency of protrusion and retraction in KO cones compared with wt (Bridgman et al., 2001). This suggests that the lifetime of protrusions may differ from KO to wt growth cones. Therefore we measured the lifetime of both filopodia and lamellipodia. Filopodia form by extension, but disappear from detection

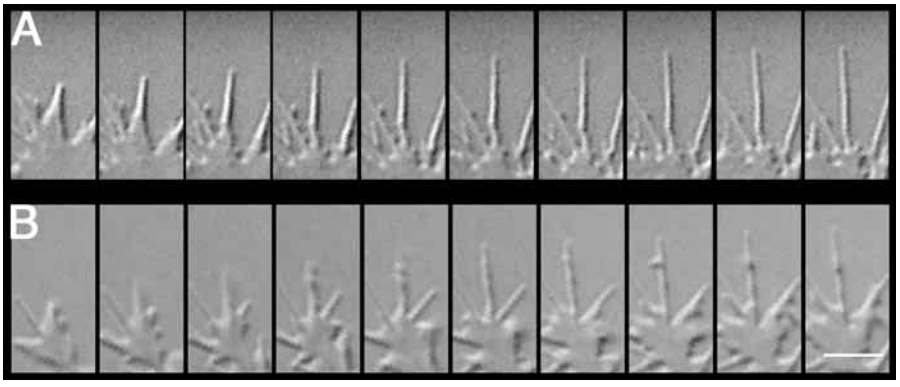


**Fig. 3.** Comparison of filopodia protrusion from wt (A) and KO (B) growth cones. (A) A sequence (10 second intervals) showing the extension of a filopodia near the leading edge of a wt growth cone. The filopodia grows in length, but some retraction of the lamellipodia at the base of the filopodia adds to the appearance of length increase. (B) A sequence as in A, but from a KO growth cone. The filopodium extends at a similar rate to the wt filopodium in A. A common feature of growing KO filopodia are the small bumps or protrusions that form. They sometimes lead to branching and appear to undergo retrograde movements. Bar, 3 μm.

through several means. They can extend and then retract, extend and be engulfed by advancing lamellipodia or extend and then move laterally to fuse with adjacent filopodia. Occasionally, filopodia also fold back and fuse with the cytoplasm proximal to their base. We only made comparisons of filopodia that extended and then retracted to ensure that we were measuring the lifetime of the actin bundle that forms the core of the filopodia. Although wt filopodia had slightly longer average lifetimes than KO filopodia, the difference was not significant (wt=202±1.7 seconds, $n$=19, KO=169±2.4 seconds, $n$=23, s.e.m., $t$-test, $P$>0.05). A similar comparison was done between lamellipodia, except that we included all modes of lamellipodial disappearance (retraction, lateral movement and filopodial extension) because they reflect a change in the organization of the actin meshwork. Wt lamellipodia had significantly longer lifetimes than KO filopodia (wt=239±2.8 seconds, $n$=18, KO=102±1.1 seconds, $n$=18; s.e.m., $t$-test, $P$<0.001). Notably, this is consistent with the observation that KO cones are smaller and have fewer lamellipodia than wt cones in time-averaged comparisons (Bridgman et al., 2001).

Retrograde flow has also been shown to affect the distribution of microtubules in the peripheral regions of growth cones. Retrograde flow transports extending microtubules rearward unless they are stabilized by interactions with actin bundles (Zhou et al., 2002; Schaefer et al., 2002). When they do interact with actin bundles the rate of peripheral extension is the sum of the microtubule polymerization rate and the retrograde flow rate (Schaefer et al., 2002). To determine if microtubule distribution was affected by the increased rate of retrograde flow observed in KO growth cones, we triple stained wt and KO growth cones for tyrosinated tubulin, F-actin and myosin IIA (Fig. 4). In comparing images from wt and KO growth cones stained for these cytoskeletal proteins, a general impression was complicated by the difference in cone shapes and the apparent lack of a distinct 'transition zone' containing actin bundles in the KO. However, upon close inspection, it was apparent that microtubules tended to more fully fill the area normally associated with a transition zone in KO cones compared with wt. Myosin IIA staining was associated with this region in both KO and wt. By contrast, the actin-rich peripheral structures appeared to contain fewer microtubule end segments in the KO. To obtain a semi-quantitative assessment of the affect of retrograde flow on microtubule distribution, we selected filopodia (or filopodia-like structures) in wt and KO cones that were associated with or partially penetrated by microtubules and then measured the distance from the microtubule tip to the distal tip of the filopodium (Fig. 4C). Microtubules penetrated further towards the tip of filopodia in the wt because the distance between microtubule ends and the tip of filopodia was significantly reduced compared with the KO (wt=3.7±2.6 μm, $n$=69; KO=4.6±2.9 μm, $n$=69; $t$-test, $P$=0.05). This is consistent with the increased retrograde flow rate of actin having an enhanced affect on distal microtubule segments associated with actin bundles of filopodia in the KO. When actin bundles are largely absent in the KO (i.e. the transition zone), the increased rate of flow has minimal affect on microtubules, and microtubules extend to fill the region.

A recent report from Dan Jay's laboratory (Diefenbach et al., 2002) presented data consistent with the idea that retrograde flow in chicken DRG neurons is driven by myosin IC. Their data also suggest that myosin II has no role in driving

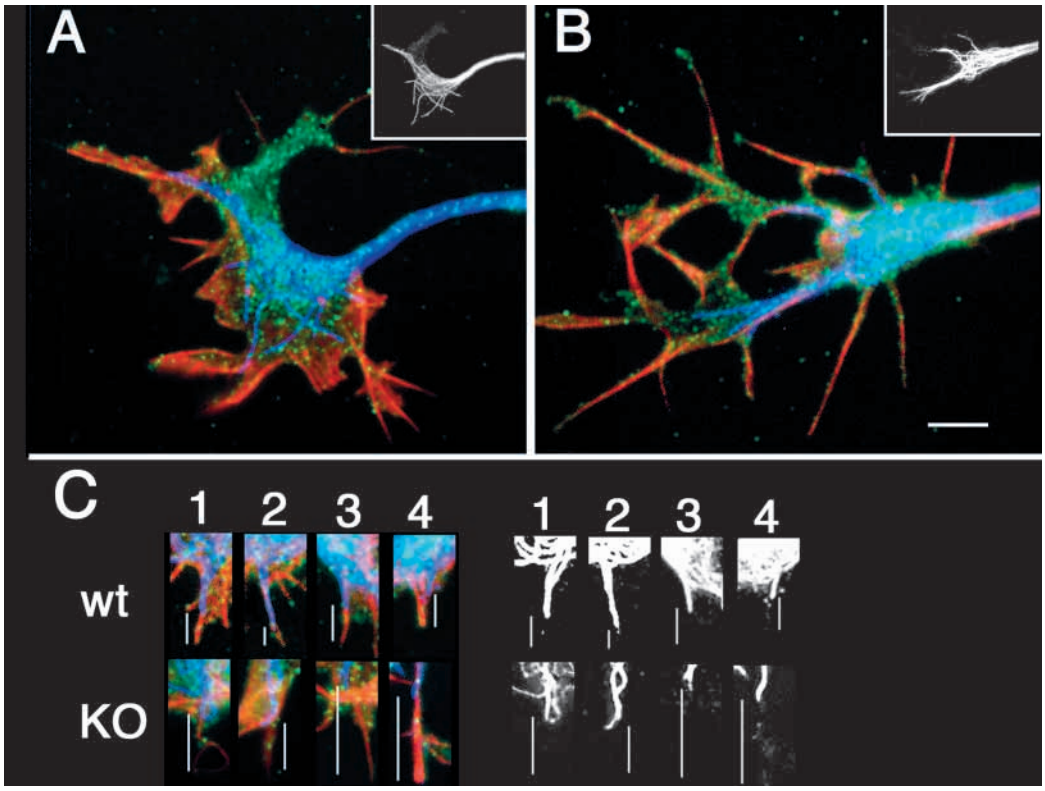


**Fig. 4.** Comparison of microtubule distribution in wt (A) and KO (B) growth cones. (A) A wt growth cone triple stained for actin (red), myosin IIA (green) and microtubules (blue). The insert shows only the microtubule staining. Microtubules penetrate the base of F-actin-rich structures. (B) A KO growth cone stained as in A. Microtubules penetrate into peripheral structures, but these often appear to have reduced staining for F-actin compared with wt. (C) Higher magnification example of multiple (1-4) microtubule ends interacting with actin containing protrusive structures. The average distance between microtubule ends and the tips of protrusive structures is greater for the KO examples. The overlap of color makes identification of microtubules difficult so the microtubule staining is also shown by itself (black and white image; contrast enhancement has produced a thickening of microtubules). B, Bar, 4.3 μm; C, the vertical Bar in No. 4=1.8 μm.

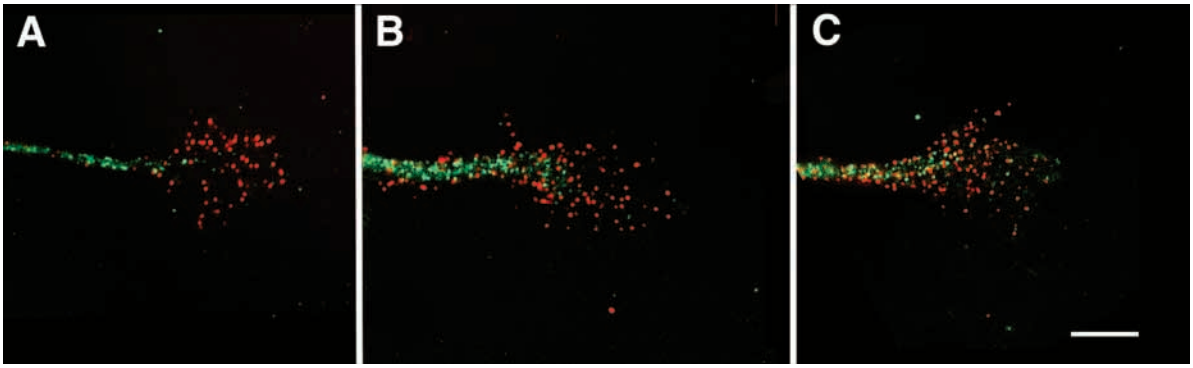


**Fig. 5.** Comparison of myosin 1C (green) and myosin IIA (red) staining in wt and KO growth cones (cold methanol fixed). (A) A KO growth cone from a SCG neuron. The myosin IC staining is mostly confined to the neurite, whereas the myosin IIA staining is distributed throughout the growth cone. Wt SCG growth cones showed a similar pattern, although the growth cones were usually larger. (B) A wt DRG growth cone shows a similar pattern of staining compared to that seen in SCG neurons (a relatively small cone was selected for comparison purposes). The intensity of the myosin IC staining appears to be elevated in the neurite compared with that observed in SCG neurons. This was consistently observed, but it is unclear if this results from thickness differences in the two types of neurites. (C) A KO DRG growth cone also shows a similar pattern and intensity of staining to the wt DRG growth cone. C, bar, 6.8 μm.

or regulating retrograde flow. To determine if myosin IC plays a role in driving retrograde flow in mouse SCG neurons, we used the same monoclonal antibody that was used in the Diefenbach study to stain SCG growth cones (Fig. 5A). We could only detect small amounts of myosin IC staining compared with myosin IIA staining (independent of fixation method) in SCG growth cones. Most of the myosin IC staining was confined to the neurite. To determine if this results from differences in cell type as opposed to species differences, we also stained mouse DRG neurons. DRG neurons stained for myosin IC were consistently slightly brighter than SCG neurons (grown from the same mouse embryos and cultured, fixed identically), but again the majority of the stain was confined to the neurite with only a few small puncta in growth cones (Fig. 5B). To determine if myosin IC is upregulated in neurons from the KO mice, we also stained SCG and DRG growth cones cultured from the KO mice. We could not detect any obvious differences in the myosin IC stain pattern or intensity compared to wt (Fig. 5). It seems unlikely that this antibody, which was made to bovine adrenal myosin IC, is less affective in detecting myosin IC in mouse compared to chicken. Thus, growth cones of mouse peripheral nerves contain only small amounts of myosin IC. This is consistent with two previous reports that showed myosin 1C protein levels in mammalian nervous tissue are low compared to other tissues (Wagner et al., 1992; Ruppert et al., 1995). In addition, myosin 1C (myr 2) does not appear to be upregulated in embryonic rodent nervous tissue (Ruppert et al., 1995).

## Discussion

Growth cones of myosin-IIB-knockout neurons show a significant increase in the maximum rate of retrograde flow. Myosin IIA drives actin filament sliding at about three-fold greater rates than myosin IIB in vitro (Kelly et al., 1996). Thus an increase in retrograde flow rate in the absence of myosin IIB is consistent with the idea that the retrograde flow rate is normally influenced by the activity of myosin IIB. In its absence this function appears to be taken over mainly by myosin IIA. Myosin IIB may normally dominate in influencing retrograde flow because it is more abundant than myosin IIA in growth cones and is concentrated in the transition zone (Rochlin et al., 1995). This would allow myosin IIB to pull and bundle actin filaments into the transition zone in a manner similar to that described for fish keratocytes (Svitkina et al., 1997). Both myosin IIA and IIB form bipolar filaments in growth cones consistent with this possibility (Bridgman, 2002). The interaction of these two myosins in growth cones is analogous to the differences observed in speed of contraction of skeletal muscle fibers. Fast and slow skeletal muscle fibers have different myosin isoforms that have different contraction speeds and ATPase activities (Wilkison et al., 1991). Some muscle fibers have mixtures of myosin isoforms and their contractile properties reflect this combination. Thus similar to muscle contraction, the contribution of the myosin IIA and IIB in influencing or driving retrograde flow can be understood in terms of their combined contributions to this activity. Also similar to muscle, the normal utilization of myosin IIB for influencing retrograde flow may reflect the efficiency of growth cone energetics. Myosin IIB has a more than two-fold lower rate of ATP hydrolysis (Kelley et al., 1996). Thus it is more efficient for the cell to affect the constant flow using myosin IIB as opposed to IIA. Seemingly in contradiction to this possibility, the outgrowth rates of myosin-IIB-knockout neurons are reduced rather than increased. However, this may reflect alterations in growth cone lamellipodial stability and traction force that contribute to growth cone advance as described in more detail below. It is possible that due to the increased energy requirements, myosin IIA activity is also more fatigable leading to greater periods of paused outgrowth. There is no indication that myosin IIA is upregulated in SCG neurons (Bridgman et al., 2001); however we cannot rule out the possibility that unidentified myosins are upregulated and contribute to the observed increase in retrograde flow rate.

It has been suggested very recently that myosin IC is the motor responsible for driving retrograde flow in growth cones (Diefenbach et al., 2002). However, mouse SCG growth cones contain little detectable myosin IC and show no obvious sign

of upregulation in KO growth cones. Although mouse DRG neurons (wt and KO) stain slightly more intensely for myosin IC, the staining pattern is similar to that observed in SCG neurons. The pattern indicates that most of the myosin IC is associated with the neurite. It is unclear if the small amount of myosin IC present at the base of the growth cone drives retrograde flow. In contrast to the more limited distribution of myosin IC, myosin IIA is relatively abundant in both mouse SCG and DRG neurons and their growth cones. Its wide distribution within the cone, and its behavior when observed in living cones is similar to that observed in noneuronal cells (Svitkina et al., 1997). The distribution and dynamic behavior are consistent with a direct role in retrograde flow. However, a direct test of a role for myosin IIA in retrograde flow has not yet been done in mouse neurons.

In the Diefenbach study, micro-CALI of myosin II or IIB did not produce significant affects on retrograde flow rates in chicken DRG neurons. However, a negative result may be hard to interpret for the following reasons. Micro-CALI of myosin II took minutes to produce easily detectable morphological effects in growth cones. If a detectable effect on retrograde flow also took several minutes, then many of the beads that were being monitored during the laser irradiation probably moved a considerable distance before being affected. This would affect the calculation of the average rate. In addition, the inactivation by microCALI may be incomplete. We note that microCALI of myosin IIB did produce an increase in the average rate of bead movement compared with the IgG control (Diefenbach et al., 2002), but the increase was not significant. If residual myosin IIB activity was present, it would presumably act to slow retrograde flow to a reduced extent. Thus a rate increase may be hard to detect. Further experiments in this system are needed to determine whether or not myosin II plays a role in retrograde flow of chicken neurons. It is possible that the myosin dependence of retrograde flow is species specific or utilizes multiple myosin types. In any case, still unexplained is the observation that retrograde flow rates exceed the actin filament sliding speeds of any of the myosins present in non-muscle cells. The dynamic contraction model (Svitkina et al., 1997) is the only current model that has the potential to explain this discrepancy (Brown and Bridgman, 2003).

The increased retrograde flow rate observed in the KO mouse SCG growth cones did not have a detectable affect on protrusion and retraction rates. This is not surprising considering that actin polymerization in filopodia and lamellipodia appears to independently regulate and respond to changes in flow rate over a wide range (Mallavarapu and Mitchison, 1999). Thus, the growth cone can compensate for the increased flow rate by increasing the actin polymerization rate. It is unclear whether or not retraction rates are dependent on retrograde flow. Similar to observations on neuroblastoma cells (Mallavarapu and Mitchison, 1999), we observed slow and fast rates of filopodia retraction in both wt and KO growth cones. Fast retraction might involve only the contractile activity of myosin IIA. Alternative mechanisms such as F-actin severing, might also contribute. Slow retraction is more likely to be influenced by the rate of retrograde flow. However, we did not observe a difference between the wt and KO in the distribution of fast and slow retractions. We also did not observe a difference when we only compared slow retraction rates.

**Table 1. Summary of tests on myosin IIB KO neurons**

| Parameter | Cultured SCG neurons from myosin IIB KO mice | Source |
|---|---|---|
| Outgrowth rate | ↓ | * |
| Filopodia-associated traction force | ↓ | ** |
| Growth cone area | ↓ | ** |
| Protrusion frequency | ↑ | ** |
| Retraction frequency | ↑ | ** |
| Protrusion area at leading edge | ↓ | ** |
| Retraction area at leading edge | NC | ** |
| Protrusion or retraction area at sides/rear | NC | ** |
| Myosin IIA expression | NC | ** |
| Actin bundles | ↓ | ** |
| Filopodia protrusion rate | NC | *** |
| Filopodia retraction rate | NC | *** |
| Filopodia lifetime | NC | *** |
| Lamellipodia lifetime | ↓ | *** |
| Retrograde flow rate | ↑ | *** |
| Microtubule + end penetration | ↓ | *** |

*Tullio et al., 2001; **Bridgman et al., 2001; ***This paper.

The lifetimes of lamellipodia, but not filopodia, were shorter in the KO compared with the wt. This is consistent with the overall morphology of the growth cones from wt and KO. KO growth cones are about half the area of wt and are more irregular in shape owing to multiple filopodial structures around their periphery (Bridgman et al., 2001; Tullio et al., 2001). This suggests that the increased rate of retrograde flow may destabilize lamellipodial structures, but not filopodia. KO growth cones have fewer transverse actin bundles in the transitional and central zones (Bridgman et al., 2001). Normally transverse bundles form in the periphery and are transported rearward by retrograde flow (Danuser and Oldenbourg, 2000). This suggests that myosin IIB is required to crosslink actin in lamellipodia to form these bundles. In their absence, lamellipodia are less stable, and this is reflected in their decreased lifetimes in the KO. A consequence of this decreased stability is less persistent growth and forward advance because normal-sized areas of lamellipodia fail to form at the leading edge (Bridgman et al., 2001). The decreased formation of large protrusive structures in the direction of growth, combined with decreased traction force of filopodia (Bridgman et al., 2001), may contribute to the slower rate of outgrowth observed in the KO neurons. The parameters that have been tested in this and other studies that contribute to the slowed outgrowth rates are qualitatively summarized in Table 1.

Consistent with the observation that retrograde flow is increased in KO growth cones, microtubules penetrate into actin-rich filopodia less than in the wt. It has been shown that microtubules in this region are influenced by retrograde flow and that their extension into the periphery reflects a balance between their polymerization rate and the rearward transport by retrograde flow (Schaefer et al., 2002). When microtubules interact with actin bundles in the growth cone periphery they can influence the direction of growth (Zhou et al., 2002). Presumably the interaction between microtubules and actin bundles leads to an increased maturation of the local cytoplasm that increases its stability and dynamics. This may include stabilization or maturation of adhesive contacts, increased actin polymerization rates and the transport of new materials to the

region (Gomez et al., 1996; Renaudin et al., 1999; Kaverina et al., 2002). Thus, if this process is inhibited, outgrowth will also be inhibited. This is consistent with the reduced formation of new protrusions that persist in the direction of growth and reduced outgrowth rates observed in the myosin IIB KO.

In conclusion, multiple isoforms of myosin II may act through several distinct but related activities to drive and regulate growth cone advance. These activities will ultimately also be important for determining the direction of growth when encountering targets that stimulate or repel the growth cone during pathfinding.

We thank Grady Phillips for excellent technical assistance. Robert S. Adelstein provided the original founders for our KO mouse colony and the GFP–myosin-IIA construct. This work was supported by NIH (RO1NS26150 to P.C.B.).

## References

**Berg, J. S., Powel, B. C. and Cheney, R. E.** (2001). A millennial myosin census. *Mol. Biol. Cell* **12**, 780-794.

**Bridgman, P. C.** (2002). Growth cones contain myosin II bipolar filament arrays. *Cell Motil. Cytoskeleton* **52**, 91-96.

**Bridgman, P. C., Dave, S., Asnes, C. F., Tullio, A. N. and Adelstein, R. S.** (2001). Myosin IIB is required for growth cone motility. *J. Neurosci.* **21**, 6159-6169.

**Bridgman, P. C., Brown, M. E. and Balan, I.** (2003). Biolistic transfection. *Methods in Cell Biology* (in press).

**Brown, J. and Bridgman, P. C.** (2003). The role of myosin II in axonal outgrowth. *J. Histochem. Cytochem.* (in press).

**Danuser, G. and Oldenbourg, R.** (2000). Probing f-actin flow by tracking shape fluctuations of radial bundles in lamellipodia of motile cells. *Biophys. J.* **79**, 191-201.

**Dembo, M. and Harris, A. K.** (1981). Motion of particles adhering to the leading edge of crawling cells. *J. Cell Biol.* **91**, 528-536.

**Diefenbach, T. J., Latham, V. M., Yimlamai, D., Liu, C. A., Herman, I. M. and Jay, D. G.** (2002). Myosin 1c and myosin IIB serve opposing roles in lamellipodial dynamics of the neuronal growth cone. *J. Cell Biol.* **158**, 1207-1217.

**Fallman, E. and Axner, O.** (1997). Design for fully steerable dual-trap optical tweezers. *Appl. Optics* **36**, 2107-2113.

**Fisher, G. W., Conrad, P. A., DeBiasio, R. L. and Taylor, D. L.** (1988). Centripetal transport of cytoplasm, actin and the cell surface in lamellipodia of fibroblasts. *Cell Motil. Cytoskeleton* **11**, 235-247.

**Forscher, P. and Smith, S. J.** (1988). Actions of cytochalsins on the organization of actin filaments and microtubules in a neuronal growth cone. *J. Cell Biol.* **107**, 1505-1516.

**Forscher, P., Lin, C. H. and Thompson, C.** (1992). Novel form of growth cone motility involving site-directed actin filament assembly. *Nature* **357**, 515-518.

**Gallo, G., Lefcort, F. B. and Letourneau, P. C.** (1997). The trkA receptor mediates growth cone turning toward a localized source of nerve growth factor. *J. Neurosci.* **17**, 5445-5454.

**Gomez, T. M., Roche, F. K. and Letourneau, P. C.** (1996). Chick sensory neuronal growth cones distinguish fibronectin from laminin by making substratum contacts that resemble focal contacts. *J. Neurobiol.* **29**, 18-34.

**Henson, J. H., Svitkina, T. M., Burns, A. R., Hughes, H. E., MacPartland, K. J., Nazarian, R. and Borisy, G. G.** (1999). Two components of actin-based retrograde flow in sea urchin coelomocytes. *Mol. Biol. Cell* **10**, 4075-4090.

**Kaverina, I., Krylyskina, O. and Small, J. V.** (2002). Regulation of substrate adhesion dynamics during cell motility. *Inter. J. Biochem. Cell Biol.* **34**, 746-761.

**Kelley, C. A., Sellers, J. R., Gard, D. L., Bui, D., Adelstein, R. S. and Baines, I. C.** (1996). *Xenopus* nonmuscle myosin heavy chain isoforms have different subcellular localizations and enzymatic activities. *J. Cell Biol.* **134**, 675-687.

**Lin, C. H. and Forscher, P.** (1995). Growth cone advance is inversely proportional to retrograde F-actin flow. *Neuron* **14**, 763-771.

**Lin, C. H., Espreafico, E. M., Mooseker, M. S. and Forscher, P.** (1996). Myosin drives retrograde F-actin flow in neuronal growth cones. *Neuron* **16**, 769-782.

**Mallavarapu, A. and Mitchison, T.** (1999). Regulated actin cytoskeleton assembly at filopodium tips controls their extension and retraction. *J. Cell Biol.* **146**, 1097-1106.

**Renaudin, A., Lehmann, M., Girault, J. A. and McKerracher, L.** (1999). Organization of point contacts in neuronal growth cones. *J. Neurosci. Res.* **55**, 458-471.

**Rochlin, M. W., Itoh, K., Adelstein, R. S. and Bridgman, P. C.** (1995). Localization of myosin IIA and B isoforms in cultured neurons. *J. Cell Sci.* **108**, 3661-3670.

**Ruppert, C., Godel, J., Muller, R. T., Kroschewski, R., Reinhard, J. and Bahler, M.** (1995). Localization of the rat myosin I molecules myr 1 and myr 2 and in vivo targeting of their tail domains. *J. Cell Sci.* **108**, 3775-3786.

**Salmon, W. C., Adams, M. C. and Waterman-Storer, C. M.** (2002). Dual-wavelength fluorescent speckle microscopy reveals coupling of microtubule and actin movements in migrating cells. *J. Cell Biol.* **158**, 31-37.

**Schaefer, A. W., Kabir, N. and Forscher, P.** (2002). Filopodia and actin arcs guide the assembly and transport of two populations of microtubules with unique dynamic parameters in neuronal growth cones. *J. Cell Biol.* **158**, 139-152.

**Suter, D. M., Errante, L. M., Belotserkovsky, V. and Forscher, P.** (1998). The Ig superfamily cell adhesion molecule, ApCAM mediates growth cone steering by substrate-cytoskeletal coupling. *J. Cell Biol.* **139**, 397-415.

**Svitkina, T. M., Verkhovsky, A. B., McQuade, K. M. and Borisy, G. G.** (1997). Analysis of the actin-myosin II system in fish epidermal keratocytes mechanism of cell body translocation. *J. Cell Biol.* **139**, 397-415.

**Theriot, J. A. and Mitchison, T. J.** (1991). Actin microfilament dynamics in locomoting cells. *Nature* **352**, 126-131.

**Thoumine, O. and Meister, J. J.** (2000). A probabilistic model for ligand-cytoskeleton transmembrane adhesion: predicting the behavior of microspheres on the surface of migrating cells. *J. Theoretical Biol.* **204**, 381-392.

**Tullio, A. N., Accili, D., Ferrans, V. J., Yu, Z. Y., Takeda, K., Grinberg, A., Westphal, H., Preston, Y. A. and Adelstein, R. S.** (1997). Nonmuscle myosin II-B is required for normal development of the mouse heart. *Proc. Natl. Sci. USA* **94**, 12407-12412.

**Tullio, A. N., Bridgman, P. C., Tresser, N. J., Chan, C. C., Conti, M. A., Adelstein, R. S. and Hara, Y.** (2001). Structural abnormalities develop in the brain after ablation of the gene encoding nonmuscle myosin II-B heavy chain. *J. Comp. Neurol.* **433**, 62-74.

**Wagner, M. C., Barylko, B. and Albanesi, J. P.** (1992). Tissue distribution and subcellular localization of mammalian myosin I. *J. Cell Biol.* **119**, 163-170.

**Wei, Q. and Adelstein, R. S.** (2000). Conditional expression of a truncated fragment of nonmuscle myosin II-A alters cell shape but not cytokinesis in HeLa cells. *Mol. Biol. Cell* **11**, 3617-3627.

**Wilkison, R. S., Nemeth, P. M., Rosser, B. W. C. and Sweeney, H. L.** (1991). Metabolic capacity and myosin expression in single muscle fibers of the garter snake. *J. Physiol.* **440**, 113-129.

**Zhou, F. Q., Waterman-Storer, C. M. and Cohan, C. S.** (2002). Focal loss of actin bundles causes microtubule redistribution and growth cone turning. *J. Cell Biol.* **157**, 839-849.